Progress In Electromagnetics Research C, Vol. 116, 13–24, 2021

Highly Isolated Two-Elements Ultra-Wideband MIMO Fractal Antenna with Multi Band-Notched Characteristics

Yong Cai[1, 2], Guangshang Cheng[1, 2], Xingang Ren[1, 2, 3, *], Jie Wu[1], Hao Ren[1], Kaihong Song[4], Zhixiang Huang[1, 4], and Xianliang Wu[1]

Abstract—This work presents a high isolation UWB-MIMO antenna with a bandwidth up to 8.6 GHz based on a Minkowski fractal structure. The proposed antenna is fed by microstrip and comprises two orthogonal monopole antennas, which delivers a decent isolation effect. Moreover, the ground is designed as two separated blocks with an I-shaped branch for improving the isolation degree between the units. The resultant isolation degree of this antenna is greater than 25 dB. Besides, the electromagnetic interference in the partial frequency band (such as Wi-Max band (3.45–4.45 GHz), WLAN band (5.1–5.8 GHz), and X-band (7.25–7.75 GHz)) is further prevented through etching a split-ring resonator (SRR) and C-slot on the unit. The antenna reflection coefficient of the UWB-MIMO antenna at the notch is 3.5 dB, which indicates that the antenna has a conspicuousness anti-interference effect. Through the above judicious design, the proposed UWB-MIMO antenna possesses a relative bandwidth of 113% (up to 8.6 GHz). The envelope correlation coefficient between antenna units is less than 0.005, and the antenna radiation efficiency is up to 80%. The results indicate that the proposed MIMO antenna meets UWB applications.

1. INTRODUCTION

Regarding the commercial wide-frequency bands of 3.1–10.6 GHz defined by the Federal Communications Commission (FCC) [1], ultra-wideband (UWB) technology has attracted intensive attention because of the advantages of broadband width, high transmission rate, low cost, etc. [2]. UWB antenna is one of the widely used components in broadband wireless communication. When it comes to short-distance and low-energy communication, resolving multipath interference is an essential issue in UWB technology [3]. Moreover, multiple-input multiple-output (MIMO) approach has been proposed to resolve the interference of signal transmission, improving the communication quality and channel capacity for such UWB applications. Besides, electromagnetic interference should be considered for UWB antenna designs since the commercial wide-frequency bands defined by the FCC cover the IEEE 802.11 Wireless Local Area Network (WLAN, e.g., 5.5 GHz).

With the development of communication equipment in the direction of multi-band work, broadband will become the trend of antenna design. More and better solutions will become the research topic of designers. Fractal antenna was originally inspired by mathematically fractal theory. Iterative self-similar design is used to maximize the length of a material in a total surface area, making fractal antennas compact and wideband [18]. The radiation characteristics of the antenna are changed periodically by using self-similarity, raising the utilization rate of space and space-filling performance effectively,

Received 4 August 2021, Accepted 19 September 2021, Scheduled 9 October 2021

* Corresponding author: Xingang Ren (xgren@ahu.edu.cn).

[1] Information Materials and Intelligent Sensing Laboratory of Anhui Province, Institute of Physical Science and Information Technology, Anhui University, Hefei 230039, China. [2] Anhui Province Key Laboratory of Target Recognition and Feature Extraction, Luan 237000, China. [3] Key Laboratory of Intelligent Computing & Signal Processing, Ministry of Education, Institute of Physical Science and Information Technology, Anhui University, Hefei 230039, China. [4] Key Laboratory of Electromagnetic Environmental Sensing, Department of Education of Anhui Province, Anhui University, Hefei 230039, China.

increasing the effective electrical size of the antenna, and the extension of the antenna surface current path to reduce the size and expand the bandwidth. There are many styles of fractal structures, which provide many possibilities for the design of new antennas, and will shine brightly in the future application prospects.

Refs. [19–22] show various methods to design fractal antennas, such as a combination of Giusepe Peano and Sierpinski Carpet [19], iterative octagon [20], bandpass FSS fractal array structure [21], and quasi-fractal slotted technology [22]. The above literature mainly adopts spatial adaptive techniques to design fractal antenna toward broadband characteristics.

In recent years, the approach to eliminate electromagnetic interference has become a research hotspot in UWB communication systems. A variety of methods have been proposed to achieve the band-notched features for UWB antennae, such as introducing a T-shaped parasitic branch [4], U-shaped slot [5], split ring resonator structure [6], and microstrip open-loop resonator to the antenna element. However, adding the above-mentioned notch structure to the traditional MIMO antenna will result in a strong coupling effect between the antenna elements. Therefore, decoupling technique should be considered during the UWB-MIMO antenna designs toward higher isolation. Moreover, the challenge of decoupling between antenna units becomes much difficult when the antenna meets the requirements of miniaturization. Therefore, the emerging techniques proposed in the literature [8–15] have been used to decrease the mutual coupling between antenna units in the UWB-MIMO antennas. In [15], a new tree structure has been proposed for broadband isolation. In [8, 9], a new branch added in the ground plane structure has been adopted to improve the antenna isolation. In [10, 11], the orthogonal polarization method has been demonstrated to reduce the mutual coupling caused by polarity diversity. The combination of the above two schemes has also been studied in [11–14] to improve the antenna isolation performance. Although the hybridized schemes could improve the isolation degree, it is difficult to adjust the current between antenna units because of combined ground, which impedes the widespread applications of such technology. It is highly desirable to adopt independent ground for UWB-MIMO antenna with high isolation. Table 1 shows the comparison of the proposed antenna and the antennas in the literature; we can see that the proposed antenna has higher isolation and radiation efficiency.

Table 1. Comparison of the proposed MIMO antenna with other reference antennas.

Reference	S_{11} (GHz)	Size (mm × mm)	Isolation (dB)	Notched band (GHz)	Total Efficiency
5	3.1–10.5	43 × 25	20	3.35–4.45 & 9–10	-
6	2.6–10.5	40 × 40	22	3.35–4.45 & 5.1–5.5	-
7	2–10.6	45 × 45	20	5.15–5.85	-
8	3.6–11	23 × 29	15	-	82%
9	2.9–20	18 × 34	22	5.1–5.8 & 7.7–8.4	75%–85%
10	4.4–7.5	35 × 35	21	-	80%
11	3–12	80 × 80	15	-	70%
12	2–12	48 × 48	15	5.1–6	-
14	3.1–10.6	32 × 32	15	-	80%
15	3.1–10.6	43 × 25	16	-	85%
Proposed	2.2–10.8	50 × 30	25	3.45–4.45 & 5.1–5.8 & 7.25–7.75	80%

In this work, we know that fractal antenna can expand the antenna bandwidth, so we propose a fractal MIMO antenna with wide-band notch performance, whose operating bandwidth is 2.2–10.8 GHz. The antenna unit is designed with the features of a Minkowski fractal structure. We adopt orthogonal polarization to improve antenna isolation; considering the inductive current between units, the newly

added floor branches are adopted to further reduce the mutual coupling between antennas, which ensures that the antenna isolation degree can reach 25 dB (the maximum isolation degree is 30 dB). In addition, the slot schemes are incorporated on the unit to avoid electromagnetic interference of antenna in Wi-Max band (3.45–4.45 GHz), WLAN band (5.1–5.8 GHz), and X downlink band (7.25–7.75 GHz).

2. ANTENNA DESIGN AND ANALYSIS

2.1. Antenna Design

The geometrical structure and corresponding parameters of the proposed UWB-MIMO antenna are shown in Figure 1. The UWB antenna was designed with two identical radiation units and two separated grounds with respective I-shaped branch. The proposed antenna size is $0.22\lambda_0 \times 0.36\lambda_0$, in which λ_0 is the operating wavelength of the antenna. When the monopole antenna iterates three times, we obtain the final model by designing the Minkowski fractal structure, as shown in Figures 1(a) and (b). This design ensures that the UWB antenna could obtain a lower operating frequency while ensuring the antenna miniaturization.

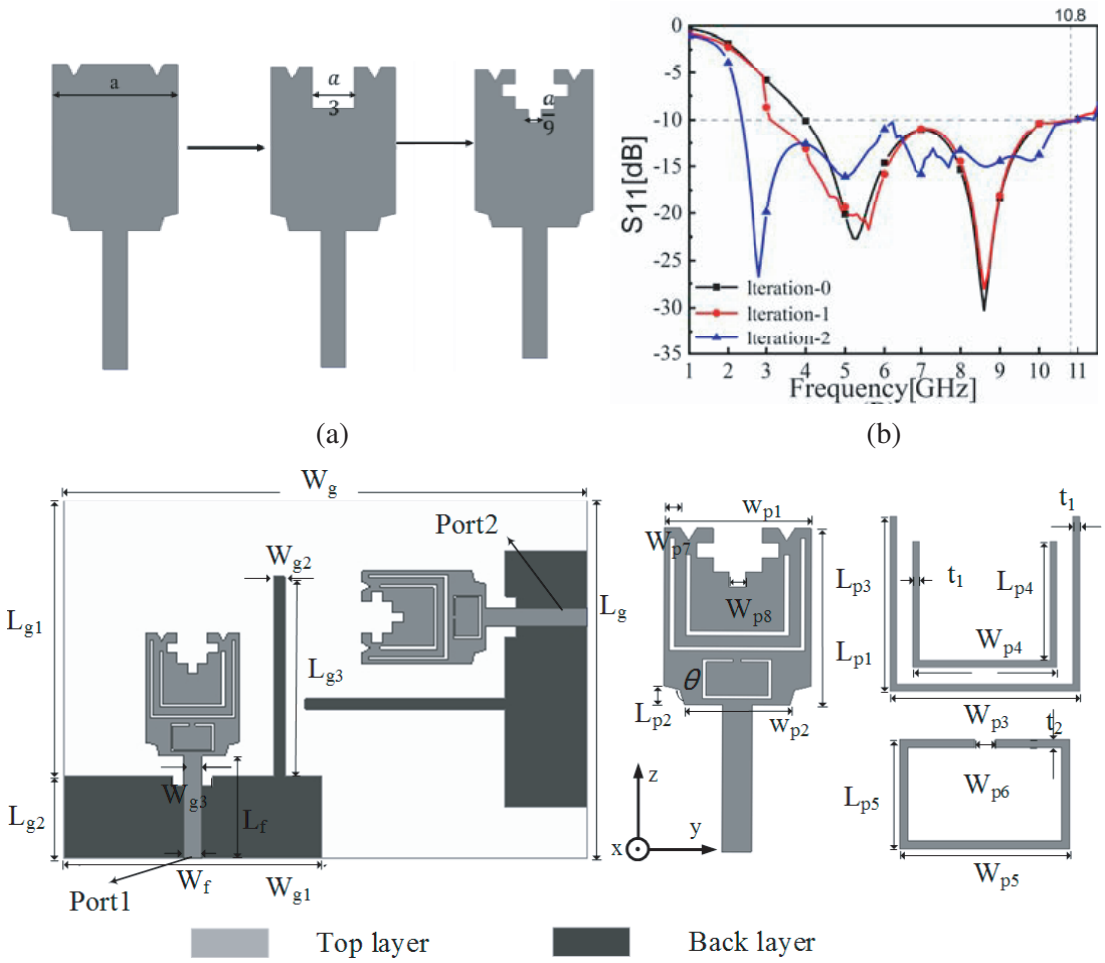

Figure 1. Illustration of the geometric structure and parameters of the UWB-MIMO antenna.

The preliminary work of the MIMO antenna was the selection of unit size and structure; to meet the demand of UWB antenna miniaturization design, monopole antenna becomes the first choice. The

formula used to calculate the lowest resonant frequency of the monopole is as follows [9]:

$$f_0 = \frac{14.4}{l_1 + l_2 + g + \frac{A_1}{2\pi\sqrt{\varepsilon_r + 1}} + \frac{A_2}{2\pi\sqrt{\varepsilon_r + 1}}} \tag{1}$$

where A_1 and A_2 indicate the area of the surface and radiation unit; l_1 and l_2 represent the length of the ground and radiation unit; g denotes the distance between the ground plane and the radiation unit, with the unit of the parameters in millimeters. In this paper, the ground plane of the antenna here is formed by a rectangular etched groove. Through etching I-shaped branches on the antenna ground plane, the antenna isolation between two units can be improved. In addition, the two units have been placed orthogonally to further enhance the isolation (as depicted in Figure 1). The antenna is fabricated on an FR4 substrate with a relative dielectric constant of 4.4.

The antenna has UWB characteristics, and it will be subject to electromagnetic interference from other frequency bands in its operating frequency band, so band-notch technology is used to avoid electromagnetic interference on the unit. In Figure 2, firstly, etching a U-shaped slot on antenna A to form antenna B, we can suppress interference in the Wi-Max band (3.45–4.45 GHz); secondly, in order to suppress the interference of the WLAN band (5.1–5.8 GHz), a U-shaped gap was etched above antenna B to form antenna C, achieving the suppression effect. Finally, considering the mutual coupling of induced current between slots, antenna D is formed by adopting split-ring resonator structures on antenna C to reject X-band downlink (7.25–7.75 GHz), completion of the design of the three band-notches. Figure 3 depicts the S_{11} curve simulated by the model used in the evolution of the unit. Meanwhile, the formula involved in Eq. (1) is: $l_1 = L_{g1} + L_{g2} l_2 = L_p{}'' 1''$, $g = L_f - L_{g2}$, $A_1 = W_{p1} L_{p1} - 12 W_{p8}^2 - W_{p7}^2 \sin 60°$, $A_2 = 2[W_{g1} L_{g2} + W_{g2} L_{g3}]$. The antenna size formula is given in Table 2 which is used to calculate the minimum working frequency of the antenna.

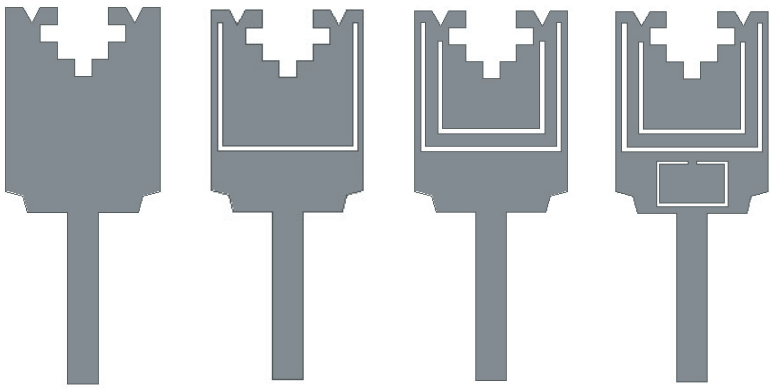

Figure 2. Several structures in the evolution of antenna.

Table 2. The geometric parameters of the UWB-MIMO antenna (unit: mm).

W_g	W_{g1}	W_{g2}	W_{g3}	W_f	W_{p1}	W_{p2}	W_{p3}
5	25	1	4	1.8	9	6.4	8
W_{p4}	W_{p7}	W_{p8}	L_g	L_{g1}	L_{g2}	L_{g3}	L_f
6	1	1	30	22	8	19.5	10
L_{p1}	L_{p2}	L_{p3}	L_{p4}	L_{p5}	t_1	t_2	
12	1.3	7.5	5.35	2.5	0.3	0.2	

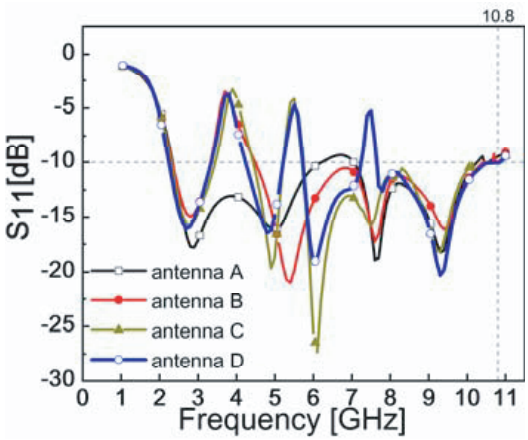

Figure 3. Simulated S_{11} in the evolution of antenna.

2.2. Influence of Ground Plane Structure

The ground plane plays an important role in antenna performance. Figure 4 shows the schematical optimization of two ground plane structures of the UWB-MIMO antenna. We can see that Ground-1 consists of two orthogonal ground planes. As shown in Figure 5(b), the isolation degree is improved through orthogonal polarization. Although the mutual coupling between antenna elements is improved, its cut-off frequency still fails to reach the standard of UWB antenna, which could not be used in practical applications. Finally, an I-shaped branch will be added to form Ground-2 (this structure can be seen as part of the radiation unit), as shown in Figure 4. Due to the I-shaped branch of the antenna, the current path of the antenna radiation will increase compared with the original one without I-shaped branch, and the working bandwidth of the antenna will also expand. So, the cut-off frequency of the antenna reaches 10.8 GHz, which meets the design requirement of the UWB antenna. Meanwhile, the starting frequency point of the antenna shifts to 2.2 GHz, further expanding the antenna bandwidth. After the adoption of the design of Ground-2, the mutual coupling between two antennas is well improved in the whole frequency band, and the isolation degree of the antenna is more than 25 dB.

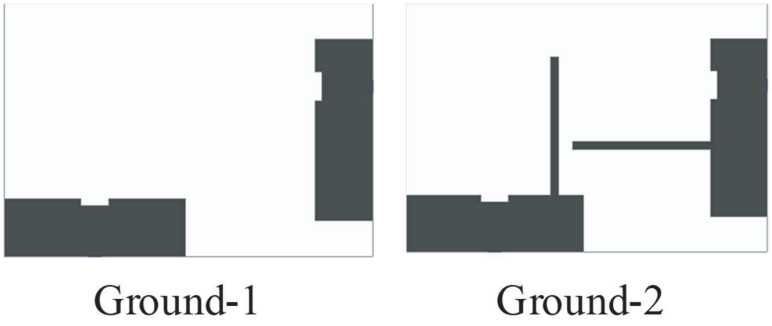

Figure 4. The optimization process of the UWB-MIMO antenna ground plane.

In order to better understand the effect of isolation between antennas, the ground current distribution is studied. As shown in Figure 6, for the antenna without I-shaped branch, the two antenna elements are orthogonal; when antenna1 is excited, the coupling current still appears in antenna2, resulting in poor isolation. However, when the hybridized structure is adopted, since this structure has become a part of the radiating element in the antenna, when antenna1 is excited, the current will be introduced into the I-shaped branch instead of antenna2, and the I-shaped branch has functioned to indirectly block the current flow to antenna2. In Figure 5(b), we can find that the isolation of the antenna is less than 25 dB when we adopt the configuration of Ground-2.

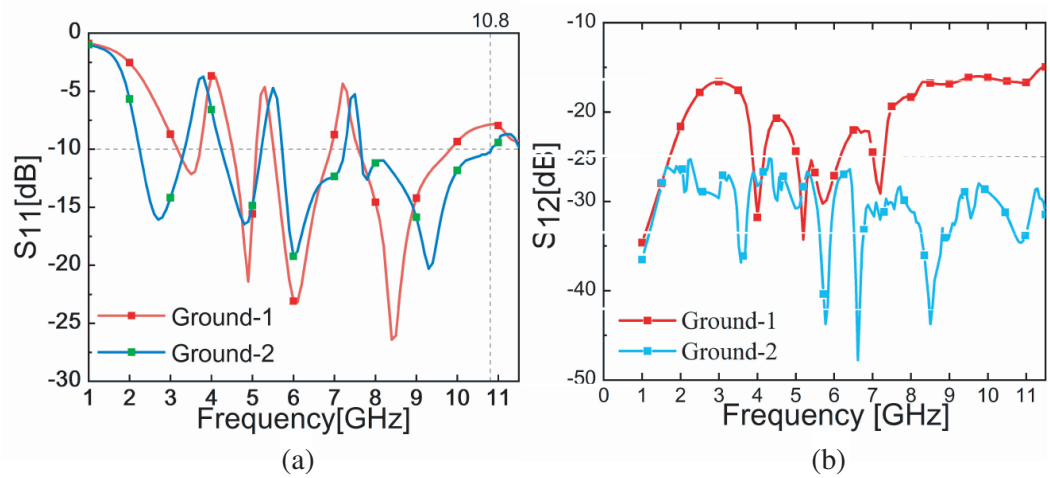

Figure 5. Simulated S-parameters of two-type ground plane structures. (a) S_{11}, (b) S_{12}.

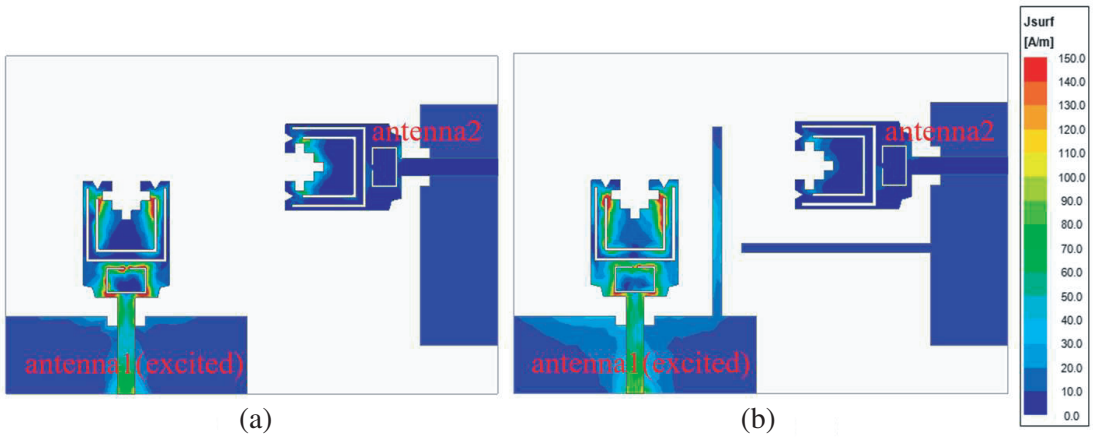

Figure 6. Current distributions of two-types ground plane structures.

2.3. Effect of C-Shaped Gap

The characteristics of the three notches bands are realized by etching a C-slot and split-ring resonator on the radiation unit. The notch characteristic of the etched groove structure on the antenna results in impedance mismatch between the feed source and radiation unit. The center frequency points of 3.8 GHz, 5.6 GHz, and 7.5 GHz are attributed to the three gaps on the antenna unit, respectively. The corresponding current distribution is shown in Figure 7. It can be seen that the surface current is respectively concentrated in the gap, which means that there is no radiation at the center frequency, and the antenna has great electromagnetic suppression across the Wi-Max band, WLAN band, and X downlink band.

Wi-Max band and WLAN band: we etch two C-slots on the radiation unit, which can be used to block the Wi-Max band (3.45–4.45 GHz) and WLAN band (5.1–5.8 GHz). This slot acts as a half guided-wavelength resonator. The formula for the length is [7]:

$$L_1 = 2L_{p3} + W_{p3} \tag{2}$$

$$L_2 = 2L_{p4} + W_{p4} \tag{3}$$

$$f = \frac{c}{2L\sqrt{\epsilon_{eff}}} \tag{4}$$

ε_{eff} is an effective dielectric constant, and c is the speed of light. The effective dielectric constant is

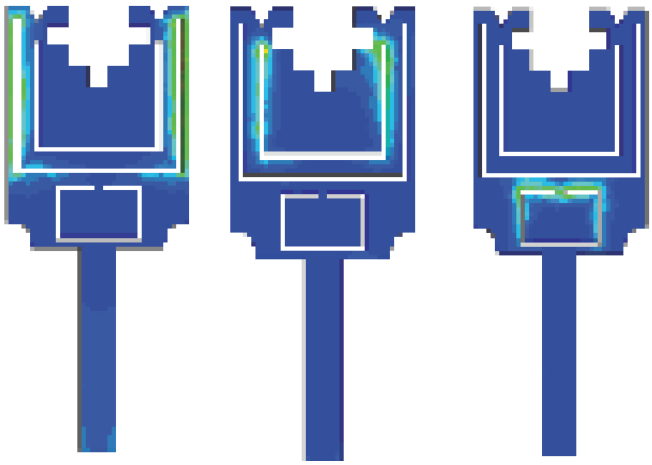

Figure 7. Current distributions of the UWB-MIMO antennas. (a) 3.8 GHz, (b) 5.6 GHz, (c) 7.5 GHz.

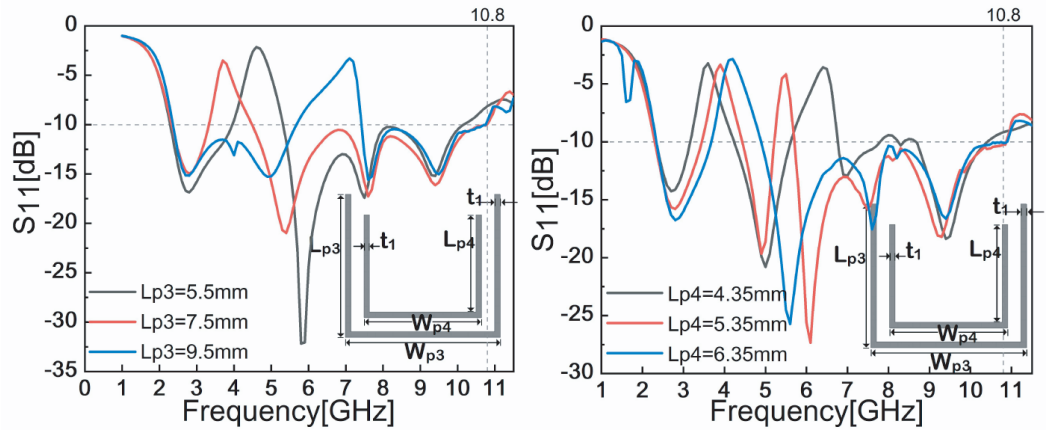

Figure 8. Simulated S-parameters against frequency for the various values of $Lp3$, $Lp4$.

half of the relative dielectric constant approximately. The material of the UWB-MIMO antenna is FR4; considering the ground effect, the effective dielectric constant is 2.7. As shown in Figure 8, for the Wi-Max band, we can see that when L_{p3} increases to 7.5 mm, the center of the notch frequency band shifts to 3.95 GHz, which meets the requirement of the Wi-Max band. Meanwhile, for the WLAN band, it can be seen that when the length L_{p4} increases to 5.35 mm, the center of notch frequency decreases to 5.5 GHz. We will get double band notches.

X-band downlink: When the radiation unit achieves the characteristic of double band notches, considering the mutual coupling of induced current between slots, the third band notch is designed by etching an SRR structure. The formula of the slot length is as follows [5]:

$$L_3 = 2(L_{p5} + W_{p5}) - W_{p6} \tag{5}$$

The band notch with 7.5 GHz as the central frequency is produced by the SRR at the bottom of the radiation unit. Figure 9 shows simulated S_{11} characteristics under different W_{p6}; as the W_{p6} decreases from 0.75 mm to 0.25 mm, the center frequency of X-band notch shifts from 8.2 GHz to 7.5 GHz. The antenna will obtain three band-notched characteristics.

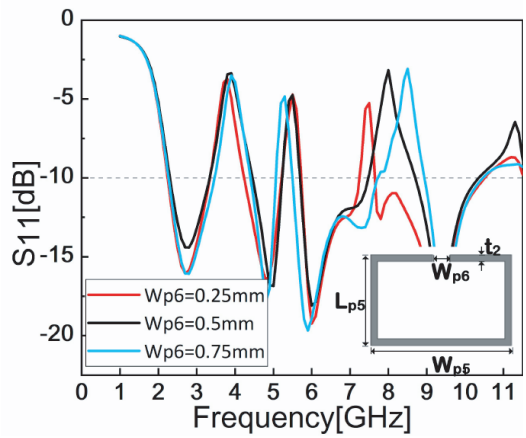

Figure 9. Simulated S_{11} characteristics under different $Wp6$ values, the other parameters unchanged.

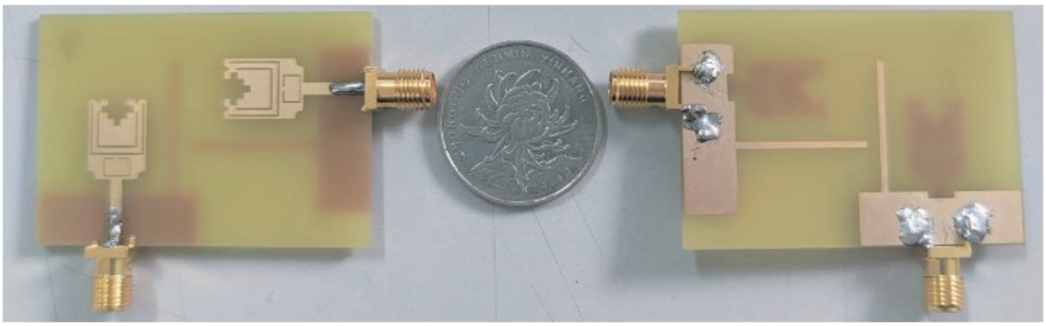

Figure 10. Prototype of the proposed UWB-MIMO fractal antenna.

3. RESULT AND DISCUSSION

We adopt the dimensions of Table 2 to fabricate the prototype as shown in Figure 10, and we adopt a vector network analyzer to extract the S parameter and verify the veracity of simulation results of the proposed UWB-MIMO antenna. In order to determine the radiation effect of the antenna, we measured the antenna pattern in a microwave dark room (Figure 12 depicts the far radiation field test of the antenna). As shown in Figure 11, the measured S_{11} and S_{12} are consistent with the simulation results. The operating frequency band of the proposed antenna is 2.2 GHz–10.8 GHz, and the isolation degree between units is more than 25 dB (most frequency bands can reach 30 dB). In addition, the three band-notched characteristics of the proposed antenna are shown in Figure 11, which can avoid electromagnetic interference from the Wi-Max band (3.45–4.45 GHz), WLAN band (5.1–5.8 GHz), and X band (7.25–7.75 GHz). Tests show that at the center frequency of the three band-notches of antenna, the reflection coefficient is only −4 dB, which indicates a good inhibition effect.

Figure 13 shows that the radiation pattern of the proposed MIMO antenna at 3.2 GHz, 4.8 GHz, 5.8 GHz, and 9.7 GHz. The measurement and simulation results of the proposed antenna are consistent and meet the omnidirectional radiation performance of the UWB antenna. When the antenna is working at low frequencies, we can see that the MIMO antenna always meets the requirement. However, at the higher frequency, due to the splitting of the radiation lobes, the antenna radiation patterns have a little deterioration. Considering the deviation between antenna welding and the actual test environment, the radiation effect of the antenna meets the design requirements.

Furthermore, in Figure 14, the antenna's total radiation efficiency has been measured; considering the effects of the antenna coupling and multi-signal recombination, we adopt the following formula to

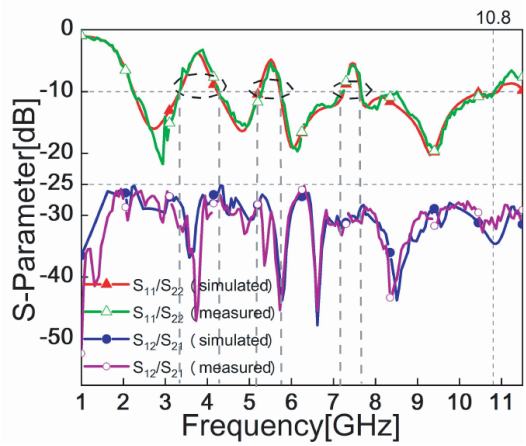

Figure 11. Measured and simulated S-parameters of the proposed UWB-MIMO antennas.

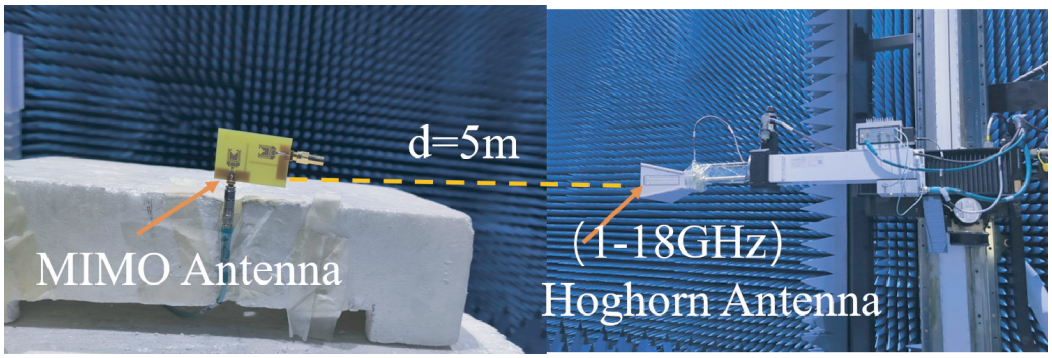

Figure 12. Test the proposed MIMO antenna far radiation field direction.

calculate [16, 17]:

$$\eta_{\Sigma} = \eta_{rad} \times \eta_{mis+coupling} \tag{6}$$

$$\eta_{mis+coupling} = 1 - |S_{11}|^2 - |S_{12}|^2 \tag{7}$$

η_{Σ} represents the total radiation efficiency of the antenna unit, and $\eta_{mis+coupling}$ represents the loss efficiency between antenna units. The radiation efficiency of the proposed antenna can reach 80% except for three notched bands, which meet the requirement of antenna design.

The performance of the proposed antenna has also been evaluated in terms of the envelope correlation coefficient (ECC); it reflects the degree of mutual coupling between antenna elements. In this paper, we adopt an orthogonal structure design antenna; in an ideal situation, if the two elements are completely orthogonal, the ECC is 0, and the calculation formula is as follows [8]:

$$ECC = \frac{\left| \iiint_{4\pi} \left[\overrightarrow{E}_1(\theta,\phi) \cdot \overrightarrow{E}_2(\theta,\phi) \right] \right|^2 d\Omega}{\iiint_{4\pi} \left| \overrightarrow{E}_1(\theta,\phi) \right|^2 d\Omega \iint_{4\pi} \left| \overrightarrow{E}_2(\theta,\phi) \right|^2 d\Omega} \tag{8}$$

Ideally, the correlation between MIMO antenna units should be zero, which means ECC = 0, but the practical limit should be less than 0.5. In Figure 13, we can see that ECC $\approx$ 0.01 of the proposed UWB-MIMO antenna meets the antenna design requirements.

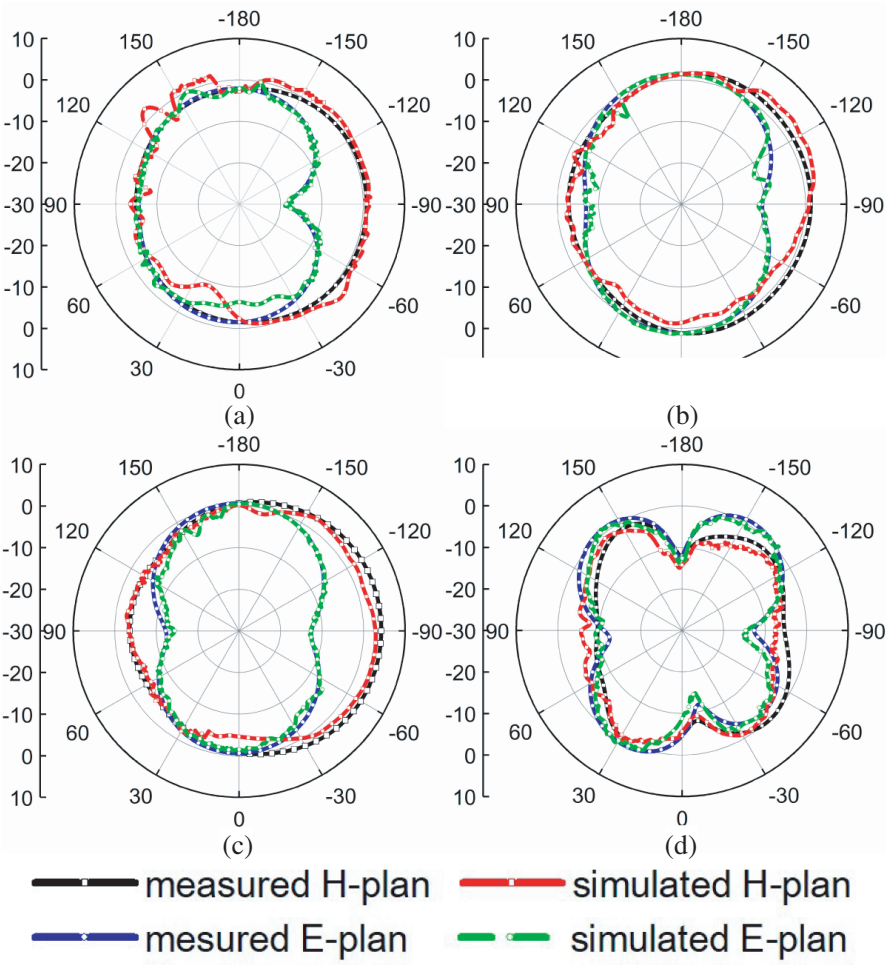

Figure 13. Measured radiation patterns of the proposed MIMO antenna at (a) 3.2 GHz, (b) 4.9 GHz, (c)5.8 GHz, (d) 9.8 GHz.

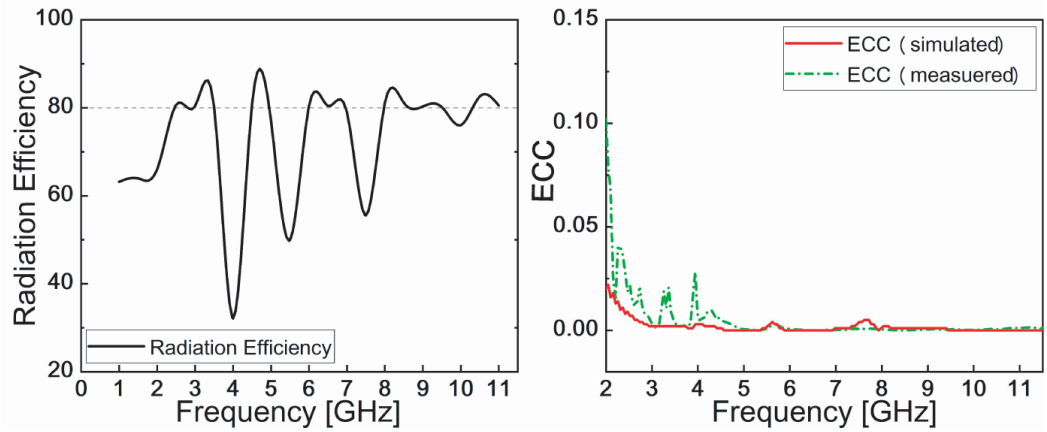

Figure 14. The ECC and efficiency for the proposed MIMO antenna.

4. CONCLUSION

A two-element UWB-MIMO antenna based on Minkowski fractal structure with three band-notched characteristics is designed by etching a U-shaped and split-ring resonator. The proposed antenna adopts an independent floor as the ground plane. Meanwhile, we can achieve the isolation more than 25 dB across 2.2–10.8 GHz with the orthogonal polarization. The measurement result shows that the reflection coefficient is approximately −4 dB when the antenna works in the band notch frequency, which means that the antenna has great anti-interference performance. Besides, through measuring the antenna radiation pattern, in whole operating frequency, the antenna has a better radiation effect. The antenna in this paper is promising for UWB-MIMO antenna applications.

ACKNOWLEDGMENT

This research is supported by the National Natural Science Foundation of China (NSFC) (62171001, 61701003, 61901002, 61901001, 61701001, U20A20164,61871001, 61971001, 6140209), of and Anhui Province (2108085MF198, 1808085QF179, 1908085QF258, 1908085QF259, 1908085QF251, the National Natural Science Fund for Excellent Young Scholars under Grant 61722101. This work is also supported by the University Synergy Innovation Program of Anhui Province (GXXT-2020-050, GXXT-2020-051), Postdoctoral Science Foundation funded project of Anhui Province (2019B348) and Open fund for Discipline Construction, Institute of Physical Science and Information Technology, Anhui University.

REFERENCES

1. Federal Communications Commission (FCC), "Revision of part 15 of the commission's rules regarding ultra-wideband transmission systems first report and order," ET Docket 98-153 FCC 02-48, adopted February 2002; released April 2002.
2. See, T. S. P. and Z. N. Chen, "An ultrawideband diversity antenna," *IEEE Transactions on Antennas and Propagation*, Vol. 57, No. 6, 1597–1605, 2009.
3. Tran, V. P. and A. Sibille, "Spatial multiplexing in UWB MIMO communications," *Electronics Letters*, Vol. 42, No. 16, 931–932, 2006.
4. Kang, L., H. Li, X. Wang, et al., "Compact offset microstrip-fed MIMO antenna for band-notched UWB applications," *IEEE Antennas and Wireless Propagation Letters*, Vol. 14, 1754–1757, 2015.
5. Mohanty, A. and S. Sahu, "High isolation two-port compact MIMO fractal antenna with Wi-Max and X-band suppression characteristics," *International Journal of RF and Microwave Computer-Aided Engineering*, Vol. 30, No. 1, 1096-110, 20197.
6. Rajkumar, S., K. T. Selvan, P. H. Rao, "Compact 4 element Sierpinski Knopp fractal UWB MIMO antenna with dual band notch," *Microwave and Optical Technology Letters*, Vol. 60, No. 4, 1023–1030, 2018.
7. Tripathi, S., A. Mohan, and S. Yadav, "A compact Koch fractal UWB MIMO antenna with WLAN band-rejection," *IEEE Antennas and Wireless Propagation Letters*, Vol. 14, 1565–1568, 2015.
8. Khan, M. S., A. Capobianco, S. M. Asif, et al., "A compact CSRR-enabled UWB diversity antenna," *IEEE Antennas and Wireless Propagation Letters*, Vol. 16, 808–812, 2017.
9. Chandel, R., A. K. Gautam, and K. Rambabu, "Tapered fed compact UWB MIMO-diversity antenna with dual band-notched characteristics," *IEEE Transactions on Antennas and Propagation*, Vol. 66, No. 4, 1677–1684, 2018.
10. Kumar Saurabh, A., P. Singh Rathore, and M. Kumar Meshram, "Compact wideband four-element MIMO antenna with high isolation," *Electronics Letters*, Vol. 56, No. 3, 117–119, 2020.
11. Gallo, M., E. Antonino-Daviu, M. Ferrando-Bataller, et al., "A broadband pattern diversity annular slot antenna," *IEEE Transactions on Antennas and Propagation*, Vol. 60, No. 3, 1596–1600, 2012.
12. Gao, P., S. He, X. Wei, et al., "Compact printed UWB diversity slot antenna with 5.5-GHz band-notched characteristics," *IEEE Antennas and Wireless Propagation Letters*, Vol. 13, 376–379, 2014.

13. Liu, L., S. W. Cheung, and T. I. Yuk, "Compact MIMO antenna for portable devices in UWB applications," *IEEE Transactions on Antennas and Propagation*, Vol. 61, No. 3, 4257–4264, 2013.
14. Ren, J., W. Hu, Y. Yin, et al., "Compact printed MIMO antenna for UWB applications," *IEEE Antennas and Wireless Propagation Letters*, Vol. 13, 1517–1520, 2014.
15. Zhang, S., Z. Ying, J. Xiong, et al., "Ultrawideband MIMO/diversity antennas with a tree-like structure to enhance wideband isolation," *IEEE Antennas and Wireless Propagation Letters*, Vol. 8, 1279–1282, 2009.
16. Yun, J. X. and R. G. Vaughan, "Multiple element antenna efficiency and its impact on diversity and capacity," *IEEE Transactions on Antennas and Propagation*, Vol. 60, No. 2, 529–539, 2012.
17. Kahn, W., "Active reflection coefficient and element efficiency in arbitrary antenna arrays," *IEEE Transactions on Antennas and Propagation*, Vol. 17, No. 5, 653–654, 1969.
18. Anguera, J., A. Andújar, J. Jayasinghe, V. V. S. S. S. Chakravarthy, P. S. R. Chowdary, J. L. Pijoan, T. Ali, and C. Cattani, "Fractal antennas: An historical perspective," *Fractal and Fractional*, Vol. 4, No. 1, 3, 2020.
19. Oraizi, H. and S. Hedayati, "Miniaturized UWB monopole microstrip antenna design by the combination of Giusepe Peano and Sierpinski Carpet fractals," *IEEE Antennas and Wireless Propagation Letters*, Vol. 10, 67–70, 2011.
20. Azari, A., "A new super wideband fractal microstrip antenna," *IEEE Transactions on Antennas and Propagation*, Vol. 59, No. 5, 1724–1727, May 2011.
21. Zheng, S., Y. Yin, J. Fan, X. Yang, B. Li, and W. Liu, "Analysis of miniature frequency selective surfaces based on fractal antenna-filter-antenna arrays," *IEEE Antennas and Wireless Propagation Letters*, Vol. 11, 240–243, 2012.
22. Hong, T., S. Gong, Y. Liu, and W. Jiang, "Monopole antenna with quasi-fractal slotted ground plane for dual-band applications," *IEEE Antennas and Wireless Propagation Letters*, Vol. 9, 595–598, 2010.